AFRL-VA-WP-TP-2002-328

NUMERICAL SIMULATIONS AND CONTROL OF THE FLOW PAST A CIRCULAR CYLINDER

MingQing Xiao
Yuan Lin
R. Chris Camphouse
James H. Myatt
Siva S. Banda

20030103 226

DECEMBER 2002

Approved for public release; distribution is unlimited.

AIR VEHICLES DIRECTORATE
AIR FORCE RESEARCH LABORATORY
AIR FORCE MATERIEL COMMAND
WRIGHT-PATTERSON AIR FORCE BASE, OH 45433-7542

REPORT DOCUMENTATION PAGE

Form Approved
OMB No. 0704-0188

1. REPORT DATE *(DD-MM-YY)*
December 2002

2. REPORT TYPE
Conference Paper Preprint

3. DATES COVERED *(From - To)*
N/A

4. TITLE AND SUBTITLE
NUMERICAL SIMULATIONS AND CONTROL OF THE FLOW PAST A CIRCULAR CYLINDER

5a. CONTRACT NUMBER
In-house

5b. GRANT NUMBER

5c. PROGRAM ELEMENT NUMBER
N/A

6. AUTHOR(S)
MingQing Xiao and Yuan Lin (Southern Illinois University)
R. Chris Camphouse, James H. Myatt, and Siva S. Banda (AFRL/VACA)

5d. PROJECT NUMBER
N/A

5e. TASK NUMBER
N/A

5f. WORK UNIT NUMBER
N/A

7. PERFORMING ORGANIZATION NAME(S) AND ADDRESS(ES)

Department of Mathematics
Southern Illinois University
Carbondale, IL 62901

Control Theory Optimization Branch (AFRL/VACA)
Control Sciences Division
Air Vehicles Directorate
Air Force Research Laboratory, Air Force Materiel Command
Wright-Patterson AFB, OH 45433-7542

8. PERFORMING ORGANIZATION REPORT NUMBER
AFRL-VA-WP-TP-2002-328

9. SPONSORING/MONITORING AGENCY NAME(S) AND ADDRESS(ES)
Air Vehicles Directorate
Air Force Research Laboratory
Air Force Materiel Command
Wright-Patterson Air Force Base, OH 45433-7542

10. SPONSORING/MONITORING AGENCY ACRONYM(S)
AFRL/VACA

11. SPONSORING/MONITORING AGENCY REPORT NUMBER(S)
AFRL-VA-WP-TP-2002-328

12. DISTRIBUTION/AVAILABILITY STATEMENT
Approved for public release; distribution is unlimited.

13. SUPPLEMENTARY NOTES
Conference paper submitted to the 33rd AIAA Fluid Dynamics Conference and Exhibit, Orlando, FL, 23-26 June 2003. This document was submitted to DTIC with color content. When the document was processed by DTIC, the color content was lost.

14. ABSTRACT
A numerical method for a finite difference approach has been established for the analysis and control of the fluid field behavior of flow past a cylinder. The discretization of the 2D Navier-Stokes equations is done over a staggered grid, the convective terms in the momentum equations are handled using a mixture of central differences and donor-cell discretization, and the Poisson equations for the pressure is solved through the successive overrelaxation (SOR) method.

We also study some open-loop and closed-loop control of the flow field by rotating the cylinder. For the open-loop control design, we mainly make use of the energy method, and for the feedback design both the energy method and the phase lock-in method are applied.

15. SUBJECT TERMS
finite difference, flow control, vortex shedding

16. SECURITY CLASSIFICATION OF:			17. LIMITATION OF ABSTRACT:	18. NUMBER OF PAGES	19a. NAME OF RESPONSIBLE PERSON (Monitor)
a. REPORT	b. ABSTRACT	c. THIS PAGE			James Myatt
Unclassified	Unclassified	Unclassified	SAR	18	19b. TELEPHONE NUMBER *(Include Area Code)* (937) 255-8491

HES&S 31-15093-1

Standard Form 298 (Rev. 8-98)
Prescribed by ANSI Std. Z39-18

Numerical Simulations and Control of the Flow Past a Circular Cylinder*

MingQing Xiao†, Yuan Lin
Department of Mathematics
Southern Illinois University
Carbondale, IL 62901

R. Chris Camphouse, James H. Myatt, Siva S. Banda
Air Force Research Laboratory, (AFRL/VACA)
Wright-Patterson AFB, OH 45433

October 12, 2002

Abstract

A numerical method for a finite difference approach has been established for the analysis and control of the fluid field behavior of flow past a cylinder. The discretization of the 2D Navier-Stokes equations is done over a staggered grid, the convective terms in the momentum equations are handled using a mixture of central differences and donor-cell discretization, and the Poisson equation for the pressure is solved through the successive overrelaxation (SOR) method.

We also study some open-loop and closed-loop control of the flow field by rotating the cylinder. For the open-loop control design, we mainly make use of the energy method, and for the feedback design both the energy method and the phase lock-in method are applied.

Keywords: Finite Difference; Flow Control; Vortex Shedding.

Extended Abstract

1 Introduction

Numerical computation is an indispensable tool for control. Computation is needed both for off-line functions such as simulation, analysis, and synthesis of control systems as well as for on-line

*Paper is submitted to the 33rd AIAA Fluid Dynamics Conference and Exhibit, Orlando, Florida 23 - 26 Jun 2003

†Research supported in part by the Summer Faculty Fellowship Program from Air Force Office of Scientific Research, 2002.

functions associated with control system implementations in embedded processors. Simulation is used to extend our capacity to reproduce and forecast physical processes on the computer. Expensive experiments are increasingly being replaced by computer simulations. Moreover, simulation enables the examination of processes that cannot be experimentally tested.

Strouhal was the first to study the periodic features produced by the movement of a cylinder body in air at low Reynolds number [18]. The understanding of the spatiotemporal dynamics of oscillatory flows has proceeded by successively considering the linearized version of Navier-Stokes equations by, among others, Joseph [17], Monkewitz, Huerre and Chomaz [21], and Yudovich [29]. Since the Navier-Stokes equations linearized about a steady-state flow is non-self-adjoint, the investigation is a difficult problem, and for the solution of the majority of questions it is necessary to use numerical methods [29].

In this paper, we use the finite difference approach to investigate wake responses under open-loop and closed-loop control. Simulations for controlling the wake flow by rotating the cylinder are provided.

2 Problem Description

The flow behavior in general can be described more or less as follows. Let $\mathbf{u}(t)$ denote the velocity field of the wake flow (here $\mathbf{u}(t)$ is the symbolic notation for a function of the space variable $\xi = (\xi_1, \xi_2, \xi_3)$). When *Re* is small (*Re* < 40), the velocity field is stable and attracts all of the orbits. In this case the flow is fully laminar. When $40 <$ *Re* < 50, steady vortices form behind the cylinder. Typically, for $t \to \infty$, $\mathbf{u}(t)$ will converge to a stationary solution

$$\mathbf{u}(t) \to \mathbf{u}^s, \qquad \text{as} \quad t \to \infty,$$

the limit solution depending on the initial condition u_0. In this case the flow is still steady.

When *Re* is grater than approximately 50, a *Hopf* bifurcation occurs, i.e.

$$\mathbf{u}(t) - \varphi(t) \to 0 \qquad \text{as} \quad t \to \infty, \tag{2.1}$$

where φ is a time-periodic solution of the system. After the Hopf bifurcation has occurred, the flow never becomes stationary again. In fact it is time periodic. In this case von Kármán vortices move in the flow direction and new vorticies appear on the downstream face of cylinder in a seemingly time-periodic manner, namely, vortex shedding.

The system of equations governing the conservation of momentum for fluid flow is known as **Navier-Stokes** equations. When combined with conservation of mass, they describes the general evolution of fluid flow. For a viscous incompressible fluid, the equations are

$$\rho\left(\frac{\partial \mathbf{u}}{\partial t} + (\mathbf{u}\cdot\nabla)\mathbf{u}\right) - \mu\Delta\mathbf{u} + \nabla\mathbf{p} = \mathbf{f} \tag{2.2}$$

$$\operatorname{div} \mathbf{u} = 0, \tag{2.3}$$

where $\rho > 0$ is the constant density of the fluid, $\nu > 0$ is the kinematic viscosity, and f represents volume forces that are applied to the fluid.

Alternatively, equation (2.2) can be considered as the *nondimensionalized form* of the Navier-Stokes equations in which case $\mathbf{u}$, $\mathbf{p}$, $\mathbf{f}$ are nondimensionalized quantities and the kinematic viscosity $\mu/\rho := \nu$ is replaced by Re^{-1}, Re representing the Reynolds number

$$Re = \frac{UL}{\nu},$$

where U and L are the typical velocity and length used for the nondimensionalization.

In this paper, we only consider the two-dimensional case and rewrite equations (2.2) in component form. Let $\mathbf{u} = (u, v)$, $\mathbf{p} = \rho p$, and $\mathbf{f} = \rho(f_x, f_y)$. Then the equations in component form read as follows:

momentum equations:

$$\frac{\partial u}{\partial t} + \frac{\partial(u^2)}{\partial x} + \frac{\partial(uv)}{\partial y} - \frac{1}{Re}\left(\frac{\partial^2 u}{\partial x^2} + \frac{\partial^2 u}{\partial y^2}\right) = f_x \tag{2.4}$$

$$\frac{\partial v}{\partial t} + \frac{\partial(uv)}{\partial x} + \frac{\partial(v^2)}{\partial y} - \frac{1}{Re}\left(\frac{\partial^2 v}{\partial x^2} + \frac{\partial^2 v}{\partial y^2}\right) = f_y, \tag{2.5}$$

continuity equation:

$$\frac{\partial u}{\partial x} + \frac{\partial v}{\partial y} = 0. \tag{2.6}$$

Let Ω be the region exterior to a circular disk with radius r. Then the open-loop or closed-loop control is acting on the circumference:

$$(u, v) = \mathbf{g(t)} \qquad \text{on } \partial\Omega. \tag{2.7}$$

3 Finite Difference Approach

Our numerical calculation is made over a collection of uniformly space discrete grid points. When central differences are used for the incompressible Navier-Stokes equations, pressure oscillations can possibly occur if all three unknown functions u, v and p, are evaluated at the same grid points [2]. There are two ways suggested for fixing the problem. One is to utilize the upwind differences, and the other is to use a staggered grid. The advantage of using the staggered grid is that a central difference approach can still be maintained. A staggered grid is illustrated in Fig.1. The pressures are calculated at the cell center, the horizontal velocities u are evaluated in the midpoints of the vertical cell edges, and the vertical velocities are computed in the midpoints of horizontal cell edges. Cell (i, j) occupies the spatial region $[(i-1)\delta x, i\delta x] \times [(j-1)\delta y, j\delta y]$, and the corresponding index (i, j) is assigned to the pressure at the cell center as well as to the u-velocity at the right edge and the v-velocity at the upper edge of this cell. The key feature is that the pressures and velocities are evaluated at different grid points so that the non-physical oscillations due to the numerical computation can be avoided.

Staggered Grid

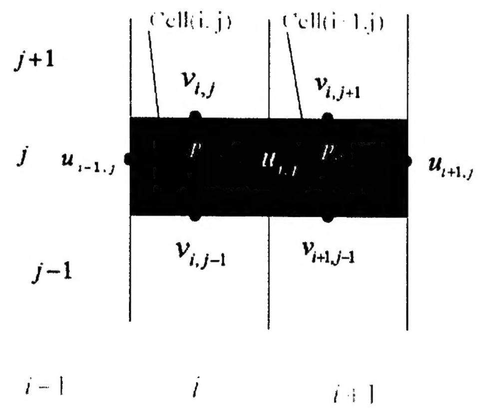

Figure 1: Stagged grid cells.

3.1 Discretization of the spatial derivatives

Let the rectangular region be

$$\Omega = [0, a] \times [0, b]$$

on which we introduce a grid. The grid is divided into i_{max} cells of equal size in the x-direction and j_{max} cells in the y-direction. We denote

$$\delta x = \frac{a}{i_{max}}, \qquad \delta y = \frac{b}{j_{max}}.$$

Then using the central difference scheme, we have

$$\left.\frac{\partial^2 u}{\partial x^2}\right|_{i,j} = \frac{u_{i+1,j} - 2u_{i,j} + u_{i-1,j}}{(\delta x)^2} \tag{3.8}$$

$$\left.\frac{\partial^2 u}{\partial y^2}\right|_{i,j} = \frac{u_{i,j+1} - 2u_{i,j} + u_{i,j-1}}{(\delta y)^2} \tag{3.9}$$

$$\left.\frac{\partial^2 v}{\partial x^2}\right|_{i,j} = \frac{v_{i+1,j} - 2v_{i,j} + v_{i-1,j}}{(\delta x)^2} \tag{3.10}$$

$$\left.\frac{\partial^2 v}{\partial y^2}\right|_{i,j} = \frac{v_{i,j+1} - 2v_{i,j} + v_{i,j-1}}{(\delta y)^2} \tag{3.11}$$

$$\left.\frac{\partial p}{\partial x}\right|_{i,j} = \frac{p_{i+1,j} - p_{i,j}}{\delta x} \tag{3.12}$$

$$\left.\frac{\partial p}{\partial y}\right|_{i,j} = \frac{p_{i,j+1} - p_{i,j}}{\delta y}. \tag{3.13}$$

3.2 Discretization of convective terms

Considering that the convective terms in the momentum equations can become dominant at high Reynolds numbers, following [11], we use a mixture of the central differences and the donor-cell discretization. In each cell (i,j), we set

$$\begin{aligned}
\left.\frac{\partial(u^2)}{\partial x}\right|_{i,j} &= \frac{1}{\delta x}\left(\left(\frac{u_{i,j}+u_{i+1,j}}{2}\right)^2 - \left(\frac{u_{i-1,j}+u_{i,j}}{2}\right)^2\right) \\
&\quad +\gamma\frac{1}{\delta x}\left(\frac{|u_{i,j}+u_{i+1,j}|}{2}\frac{(u_{i,j}-u_{i+1,j})}{2} - \frac{|u_{i-1,j}+u_{i,j}|}{2}\frac{(u_{i-1,j}-u_{i,j})}{2}\right);
\end{aligned}$$

$$\begin{aligned}
\left.\frac{\partial(uv)}{\partial y}\right|_{i,j} &= \frac{1}{\delta y}\left(\frac{(v_{i,j}+v_{i+1,j})}{2}\frac{(u_{i,j}+u_{i,j+1})}{2} - \frac{(v_{i,j-1}+v_{i+1,j-1})}{2}\frac{(u_{i,j-1}+u_{i,j})}{2}\right) \\
&\quad +\gamma\frac{1}{\delta y}\left(\frac{|v_{i,j}+v_{i+1,j}|}{2}\frac{(u_{i,j}-u_{i,j+1})}{2} - \frac{|v_{i,j-1}+v_{i+1,j-1}|}{2}\frac{(u_{i,j-1}-u_{i,j})}{2}\right);
\end{aligned}$$

$$\begin{aligned}
\left.\frac{\partial(uv)}{\partial x}\right|_{i,j} &= \frac{1}{\delta x}\left(\frac{(u_{i,j}+u_{i,j+1})}{2}\frac{(v_{i,j}+v_{i+1,j})}{2} - \frac{(u_{i-1,j}+u_{i-1,j+1})}{2}\frac{(v_{i-1,j}+v_{i,j})}{2}\right) \\
&\quad +\gamma\frac{1}{\delta x}\left(\frac{|u_{i,j}+u_{i,j+1}|}{2}\frac{(v_{i,j}-u_{i+1,j})}{2} - \frac{|u_{i-1,j}+u_{i-1,j+1}|}{2}\frac{(v_{i-1,j}-v_{i,j})}{2}\right);
\end{aligned}$$

$$\begin{aligned}
\left.\frac{\partial(v^2)}{\partial y}\right|_{i,j} &= \frac{1}{\delta y}\left(\left(\frac{v_{i,j}+v_{i,j+1}}{2}\right)^2 - \left(\frac{v_{i,j-1}+v_{i,j}}{2}\right)^2\right) \\
&\quad +\gamma\frac{1}{\delta y}\left(\frac{|v_{i,j}+v_{i,j+1}|}{2}\frac{(v_{i,j}-u_{i,j+1})}{2} - \frac{|v_{i,j-1}+v_{i,j}|}{2}\frac{(v_{i,j-1}-v_{i,j})}{2}\right),
\end{aligned}$$

where γ is a parameter between 0 and 1. During the simulation, the γ is chosen to be 0.9.

3.3 Iteration for solving the Poission equation for pressure

We use a forward difference for the time discretization. Thus the momentum equations become:

$$u^{(n+1)} = u^{(n)} + \delta t\left[\frac{1}{Re}\left(\frac{\partial^2 u}{\partial x^2}+\frac{\partial^2 u}{\partial y^2}\right) - \frac{\partial(u^2)}{\partial x} - \frac{\partial(uv)}{\partial y} + f_x\right] - \delta t\frac{\partial p}{\partial x} \tag{3.14}$$

$$v^{(n+1)} = v^{(n)} + \delta t\left[\frac{1}{Re}\left(\frac{\partial^2 v}{\partial x^2}+\frac{\partial^2 v}{\partial y^2}\right) - \frac{\partial(uv)}{\partial x} - \frac{\partial(v^2)}{\partial y} + f_y\right] - \delta t\frac{\partial p}{\partial y}. \tag{3.15}$$

Let

$$F^{(n)} = u^{(n)} + \delta t\left[\frac{1}{Re}\left(\frac{\partial^2 u}{\partial x^2}+\frac{\partial^2 u}{\partial y^2}\right) - \frac{\partial(u^2)}{\partial x} - \frac{\partial(uv)}{\partial y} + f_x\right]^{(n)} \tag{3.16}$$

$$G^{(n)} = v^{(n)} + \delta t\left[\frac{1}{Re}\left(\frac{\partial^2 v}{\partial x^2}+\frac{\partial^2 v}{\partial y^2}\right) - \frac{\partial(uv)}{\partial x} - \frac{\partial(v^2)}{\partial y} + f_y\right]^{(n)}. \tag{3.17}$$

We then set

$$u^{(n+1)} = F^{(n)} - \delta t \frac{\partial p^{(n+1)}}{\partial x} \tag{3.18}$$

$$v^{(n+1)} = G^{(n)} - \delta t \frac{\partial p^{(n+1)}}{\partial y}. \tag{3.19}$$

Making use of the continuity equation, we have the Possion equation for the pressure $p^{(n+1)}$ at time t_{n+1}:

$$\frac{\partial^2 p^{(n+1)}}{\partial x^2} + \frac{\partial^2 p^{(n+1)}}{\partial y^2} = \frac{1}{\delta t}\left(\frac{\partial F^{(n)}}{\partial x} + \frac{\partial G^{(n)}}{\partial y}\right). \tag{3.20}$$

Using central difference for the Laplacian operator, we obtain

$$\frac{p_{i+1,j}^{(n+1)} - 2p_{i,j}^{(n+1)} + p_{i-1,j}^{(n+1)}}{(\delta x)^2} + \frac{p_{i,j+1}^{(n+1)} - 2p_{i,j}^{(n+1)} + p_{i,j-1}^{(n+1)}}{(\delta y)^2} \tag{3.21}$$

$$= \frac{1}{\delta t}\left(\frac{F_{i,j}^{(n)} - F_{i-1,j}^{(n)}}{\delta x} + \frac{G_{i,j}^{(n)} - G_{i,j-1}^{(n)}}{\delta y}\right). \tag{3.22}$$

An iterative method, called successive overrelaxation (SOR), is applied to solve the above discretized equation:

$$\begin{aligned} p_{i,j}^{it+1} &= p_{i,j}^{it} + \omega\left(\frac{1}{\frac{2}{(\delta x)^2} + \frac{2}{(\delta y)^2}} - p_{i,j}^{it}\right) \\ &\cdot\left(\frac{p_{i+1,j}^{it} + p_{i-1,j}^{it+1}}{(\delta x)^2} + \frac{p_{i,j+1}^{it} + p_{i,j-1}^{it+1}}{(\delta y)^2} - \frac{1}{\delta t}\left(\frac{F_{i,j}^{(n)} - F_{i-1,j}^{(n)}}{\delta x} + \frac{G_{i,j}^{(n)} - G_{i,j-1}^{(n)}}{\delta y}\right)\right), \end{aligned}$$

where $\omega \in [0, 2]$ is a parameter. The residual is defined to be

$$r_{i,j}^{it} = \frac{p_{i+1,j}^{it} - 2p_{i,j}^{it} + p_{i-1,j}^{it}}{(\delta x)^2} + \frac{p_{i,j+1}^{it} - 2p_{i,j}^{it} + p_{i,j-1}^{it}}{(\delta y)^2} - \frac{1}{\delta t}\left(\frac{F_{i,j}^{(n)} - F_{i-1,j}^{(n)}}{\delta x} + \frac{G_{i,j}^{(n)} - G_{i,j-1}^{(n)}}{\delta y}\right).$$

The iteration is terminated when either a specified number of iterations has been reached or the norm of the residual is smaller than a specified tolerance. In the simulation, $\omega = 1.7$.

3.4 Stability issue

One of common methods to ensure stability of the numerical algorithm and prevent the numerical solution from generating non-physical oscillations is to set the time step to meet three conditions:

$$\delta t < \frac{Re}{2}\left(\frac{1}{(\delta x)^2} + \frac{1}{(\delta y)^2}\right)^{-1}, \quad \delta t < \frac{\delta x}{|u_{max}|}, \quad \delta t < \frac{\delta y}{|v_{max}|}. \tag{3.23}$$

We follow reference [25] and use an adaptive stepsize control:

$$\delta t := \tau \min\left(\frac{Re}{2}\left(\frac{1}{(\delta x)^2} + \frac{1}{(\delta y)^2}\right)^{-1}, \frac{\delta x}{|u_{max}|}, \frac{\delta y}{|v_{max}|}\right), \tag{3.24}$$

where the factor $\tau \in [0, 1]$ is a safety factor. In the simulation, we choose $\tau = 0.5$.

4 Simulation with Open-loop Control

The simulations are based on the solution of the following Navier-Stokes equations:

$$\frac{\partial \mathbf{u}}{\partial t} = -\nabla p - (\mathbf{u} \cdot \nabla)\mathbf{u} + \frac{1}{Re}\nabla^2 \mathbf{u} \qquad \text{in } \Omega, \tag{4.25}$$

$$\text{div}\, \mathbf{u} = 0 \qquad \text{in } \Omega, \tag{4.26}$$

$$\mathbf{u} = s(x_2, -x_1)/r \qquad \text{on } \partial\Omega, \tag{4.27}$$

$$\mathbf{u} = \mathbf{U}_\infty, \qquad \text{on } \Gamma_1 \tag{4.28}$$

$$\mathbf{u} = 0 \qquad \text{on } \Gamma_2, \Gamma_3, \tag{4.29}$$

where s is the angular speed (possibly time-dependent) of the cylinder, and $\mathbf{U}_\infty = (u_\infty, 0)$ is the free stream velocity.

5 Simulation with Closed-loop Control

It is well-known that the von Kármán vortex street induces a strong unsteady transverse periodic force on the cylinder which can lead to cylinder oscillations with large amplitudes. Such oscillations can cause structural damage and structure failure in applications. A means of altering the wake structure through feedback control in order to reduce or eliminate such vibrations is of practical importance. One approach is to introduce feedback into the system with one or more sensors and actuators so that the combined system is stable. Here we study a simple approach.

We assume that we can measure the upstream velocity away from the cylinder. In our simulations, we use the average of the speeds of three cells (which are about 1.5 units ahead of the cylinder) to serve as known information. Then we place five sensors evenly on the downstream semicircle of the cylinder. Let us denote these five sensing velocities as (u_i, v_i). Let the active control be

$$\mathbf{g}(t) = G \sin(2\pi f t)(y, -x)/r \qquad \text{on } \partial\Omega \tag{5.30}$$

where G is the feedback gain, r is the radius of the cylinder, and f is a selected frequency. Here the frequency f can be chosen such that it can reduce the vibration of the cylinder. For example, f can be picked to be larger than the shedding frequency to avoid the occurrence of resonance. The feedback gain G is set to be the following. Let $T = 1/f$ and

$$\Delta(t_n) := \sum_i \sqrt{(u_i(t_n) - u_i(t_n - T))^2 + (v_i(t_n) - v_i(t_n - T))^2}. \tag{5.31}$$

Then at $t = 0$ we set $G = U_\infty$. When the feedback is turned on, after one period T we set

$$G(t) = G(t_n) + \Delta(t_n) \quad \text{for } t_n < t < t_{n+1} := T + t_n \tag{5.32}$$

if the free stream velocity remains the same. Otherwise reset G to be the free stream velocity. The purpose is to let the feedback increase the amplitude automatically until the flow is locked in a periodic solution with the period T. In this case the cylinder will be oscillated at a desirable

frequency. The numerical simulations of the closed-loop design are carried out. The simulations are done in multiple phases. [The selected frequency (or forced frequency) is $f = 0.25$.] The natural frequency (without the control) is about 0.21. In phase 1, $U_\infty = 1$ and $Re = 100$, and in phase 2, $U_\infty = 5$ and $Re = 500$. In phase 3, $U_\infty = 1$ and $Re = 100$, which are the same values as in phase 1.

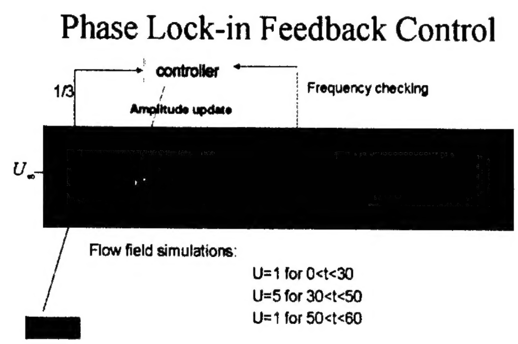

Figure 2: Phase Lock-in Feedback

6 Outline of Simulation Results

A sequence of numerical simulations have been obtained. The simulations consists of the flow behaviors (1) without control; (2) with open-loop control; (3) with closed-loop control. We here only provide some results of the simulations (Fig.3-6).

References

[1] G. Addington, J. Hall and J. Myatt. Reduced order modeling applied to reactive flow control. *AIAA 2002-4807.*

[2] J. D. Anderson. Computational Fluid Dynamics. McGraw-Hill, Inc., 1995.

[3] B. Pier. On the frequency selection of finite-amplitude vortex shedding in the cylinder wake. *J. Fluid Mech.* Vol. 458, pp. 407-417, 2002.

[4] A. J. Chorin and J. E. Marsden. A Mathematical Introduction to Fluid Mechanics. *Springer-Verlag*, third edition, 1993.

[5] R. L. Devaney. A First Course in Chaotic Dynamical Systems. *Reading, Mass.*, Addison-Wesley, 1992.

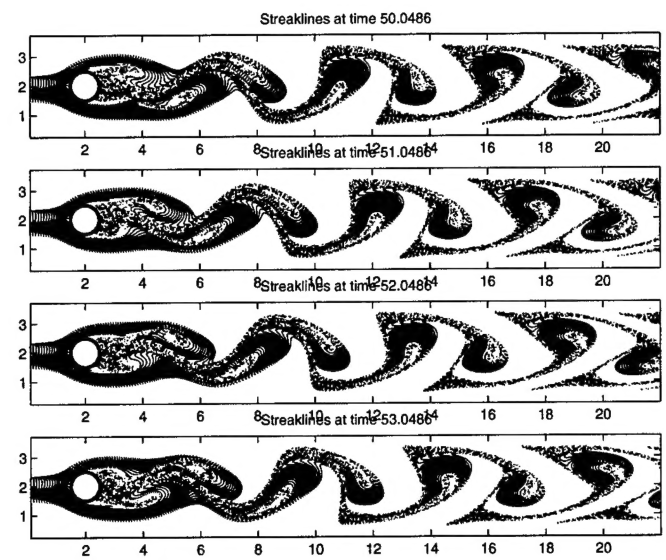

Figure 3: Streakline in a vortex shedding period without control

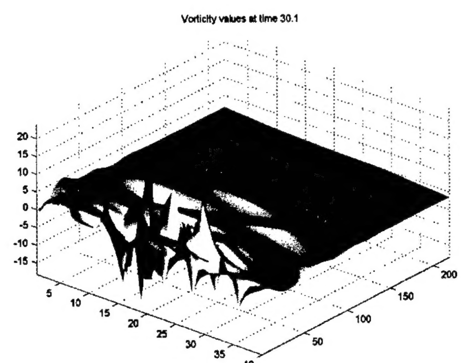

Figure 4: Vorticity distribution at $Re = 100$ and $time \approx 30$ when the cylinder is rotated in a constant speed =1

Open loop Control: Cylinder Rotation

Reynolds number	Rotating speed	Ave. Drag reduced	Lift coefficient increased
100	0.85	22.09 %	4.63
200	0.95	29.85 %	5.47
300	1.00	31.96 %	5.80
500	1.20	28.42 %	8.09

Figure 5: Drag and lift coefficients with open-loop control.

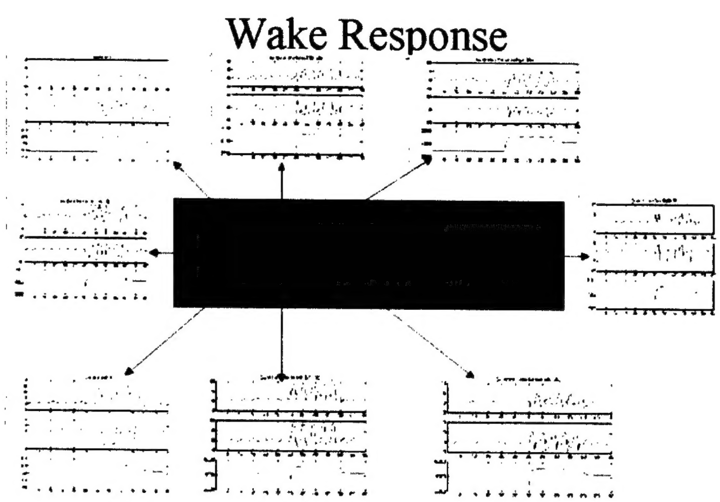

Figure 6: Wake response in different locations

[6] T. Dubois, F. Jauberteau, and R. Temam. Dynamic multilevel methods and the numerical simulation of turbulence. *Cambridge, UK*, New York, Cambridge University Press, 1999.

[7] M. Farkas. Periodic Motions. *Springer*, New York, 1994.

[8] C. Foias, O. Manley, R. Rosa, and R. Temam. Navier-Stokes Equations and Turbulence. *Cambridge University Press*, 2001.

[9] E. A. Gillies. Low-dimensional control of the circular cylinder wake. *J. Fluid Mech.* Vol. 371, pp. 157-178, 1998.

[10] P. Glendinning. Stability, Instability and Chaos. *Cambridge University Press*, 1994.

[11] M. Griebel, T. Dornseifer, and T. Neunhoeffer. Numerical Simulation in Fluid Dynamics. *SIAM*, Philadelphia, 1998.

[12] C. Grebogi and Y. C. Lai. Controlling chaotic dynamical systems. *System Control Lett.*, **31**, no. 5, pp. 307-312, 1997.

[13] W. R. Graham, J. Peraire, and K. Y. Tang. Optimal control of vortex shedding using low order models Part I: open-loop model development. *Int. J. for Num. Methods in Engr.*, 44(7), pp. 973-990, 1999.

[14] M. Gad-el-Hak. Flow control: the future *J. of Aircraft*, Vol. 38, No. 3, 2001.

[15] J. O. Hinze. Turbulence. *McGraw-Hill, Inc.*, second edition, 1987.

[16] D. A. Jones and E. S. Titi. Determining finite volume elements for the 2D Navier-Stokes equations. *Physica*, **60D**, pp. 165-174, 1992.

[17] D. D. Joseph. Hydrodynamic stability and bifurcation. *In Hydrodynamic Instabilities and the Transition to Turbulence*, edited by H. L. Swinney and J. P. Gollub, second edition, Springer-Verlag, 1985.

[18] L. Landau and E. Lifshitz. Fluid Mechanics. *Pergamon*, Oxford, 1959.

[19] X. Ma and G. E. Karniadakis. A low-dimensional model for simulating three-dimensional cylinder flow. *J. Fluid Mech.* Vol. 458, pp. 181-190, 2002.

[20] J. E. Marsden and M. F. McCracken. The Hopf Bifurcation and Its Applications. *Springer-Verlag*, 1976.

[21] P. Monkewitz, P. Huerre, and J. M. Chomaz. Global linear stability analysis of weakly non-parallel shear flows. *J. Fluid Mech.* Vol. 251, pp. 1-20, 1993.

[22] P. J. Schmid and D. S. Henningson. Stability and Transition in Shear Flows. *Springer-Verlag*, 2001.

[23] M. Schumm, E. Berger and P. A. Monkewitz. Self-excited oscillations in the wake of two-dimensional bluff bodies and their control. *J. Fluid Mech.* Vol. 271, pp. 17-53, 1994.

[24] P. T. Tokumaru and P. E. Dimotakis. Rotary oscillation control of a cylinder wake. *J. Fluid Mech.* Vol. 224, pp. 77-90, 1991.

[25] M. Tome and S. McKee. GENSMAC: A computational marker and cell method for free surface flows in general domains. *J. Comput. Phys.*, 110, 171-186, 1994.

[26] K. Roussopoulos. Feedback control of vortex shedding at low Reynolds numbers. *J. Fluid Mech.* Vol. 248, pp. 267-296, 1993.

[27] M. Xiao, M. Novy, J. Myatt, and S. Banda. A Rotary Control of the Circular Cylinder Wake: An Analytic Approach. *AIAA*, 2002.

[28] S. Wiggins. Introduction to Applied Nonlinear Dynamical Systems and Chaos. *Springer-Verlag*, Berlin, 1990.

[29] V. I. Yudovich. The Linearization Method in Hydrodynamical Stability Theory. *American Mathematical Society*, Volume 74, 1989.